

pubs.acs.org/jcim Article

On the Possibility That Bond Strain Is the Mechanism of RING E3 Activation in the E2-Catalyzed Ubiquitination Reaction

Jay-Anne K. Johnson and Isaiah Sumner*



Cite This: https://doi.org/10.1021/acs.jcim.2c00423



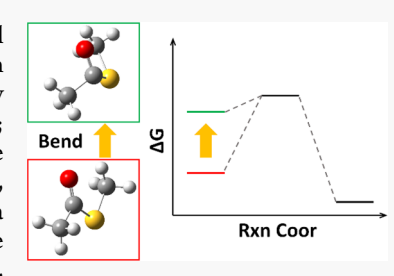
ACCESS

Metrics & More

Article Recommendations

Supporting Information

ABSTRACT: Ubiquitination is a type of post-translational modification wherein the small protein ubiquitin (Ub) is covalently bound to a lysine on a target protein. Ubiquitination can signal for several regulatory pathways including protein degradation. Ubiquitination occurs by a series of reactions catalyzed by three types of enzymes: ubiquitin activating enzymes, E1; ubiquitin conjugating enzymes, E2; and ubiquitin ligases, E3. E2 enzymes directly catalyze the transfer of Ub to the target protein—the RING E3 improves the efficiency. Prior to its transfer, Ub is covalently linked to the E2 via a thioester bond and the Ub~E2 conjugate forms a quaternary complex with the RING E3. It is hypothesized that the RING E3 improves the catalytic efficiency of ubiquitination by placing the E2~Ub conjugate in a "closed" position,



which tensions and weakens the thioester bond. We interrogate this hypothesis by analyzing the strain on the thioester during molecular dynamics simulations of both open and closed E2~Ub/E3 complexes. Our data indicate that the thioester is strained when the E2~Ub conjugate is in the closed position. We also show that the amount of strain is consistent with the experimental rate enhancement caused by the RING E3. Finally, our simulations show that the closed configuration increases the populations of key hydrogen bonds in the E2~Ub active site. This is consistent with another hypothesis stating that the RING E3 enhances reaction rates by preorganizing the substrates.

1. INTRODUCTION

Many cellular processes in eukaryotes are initiated by attaching a small protein, ubiquitin (Ub), to a target protein. 1-4 This process may involve a single ubiquitin or a polyubiquitin chain. Ubiquitin is attached through a series of enzymatic reactions catalyzed by ubiquitin activating (E1), ubiquitin conjugating (E2), and ubiquitin ligase (E3) enzymes. At the E2 step, Ub is covalently bound to the E2 through a thioester linkage. The C-terminal glycine on Ub bonds to a cysteine side chain on the E2. Next, a lysine side chain on the target protein attacks the thioester carbonyl carbon to form a zwitterionic, tetrahedral intermediate. Finally, the intermediate collapses, an isopeptide bond forms between the Ub and the target, and the E2 is released. This process is shown in Figure 1, where the target protein is also a Ub. This reaction is assisted by an E3 ligase.

The E3 serves to recruit the target protein and catalyzes the final Ub transfer. There are several families of E3 enzymes. Homologous to E6AP C-terminus (HECT) and RING between RING (RBR) E3 ligases transfer the Ub to a target in a two-step process: They first move the Ub from the E2 to a cysteine on the E3 and then move the Ub to its final target. Really interesting new gene/U-box (RING) E3 ligases, the focus of this paper, catalyze the direct transfer of Ub from the E2 to its target and do not change any chemical steps. Sec.

RING E3s are the largest class of E3 enzymes⁷ and are thought to activate or prime the E2~Ub conjugate for Ub transfer by orienting the substrate lysine in an ideal attack position and by immobilizing the thioester linkage between the E2 and the Ub.^{5,8} This preorganization occurs when the RING E3 places

the E2~Ub complex in the closed position (see Figure 2).^{6,9-17} It has been shown recently that Ub transfer occurs exclusively when the E2~Ub is in the closed position.¹⁶ Closed conformations have also been observed in RING E3 complexes for other Ub-like (Ubl) proteins like SUMO and Nedd8,^{18,19} which hints at a universal mechanism. In addition to preorganization, another intriguing hypothesis for the mechanism of E3 activation is that the closed position strains the thioester bond, "like tensioning a spring", 6 which makes it easier to break.

In this study, we test both the strain and preorganization hypotheses using molecular dynamics (MD) simulations. Our model E2 is Ubc13, which forms K63-linked polyubiquitin chains, that is, Ub is also the target protein. K63-linked chains are not directly involved in protein degradation, L1,22 but instead are involved in other processes like inflammation response and DNA repair. Our simulations also include a Ub E2 variant (UEV), which orients the substrate Ub so that lysine 63 (K63) is positioned for attack. Finally, our model E3 is the RNF4 RING domain. We monitor the thioester strain in the Ubc13~Ub/UEV complex in the open and closed positions. We also observe

Special Issue: Advancing Women in Chemistry

Received: April 12, 2022



Figure 1. This is a simplified reaction scheme of an E2-catalyzed formation of a polyubiquitin chain. The substrate ubiquitin is marked Ub*. In the first step, the E2 and Ub are bound via a thioester linkage. The reaction then proceeds through a zwitterionic, tetrahedral intermediate, before it collapses into the products—the regenerated E2 enzyme and an isopeptide-linked Ub chain.

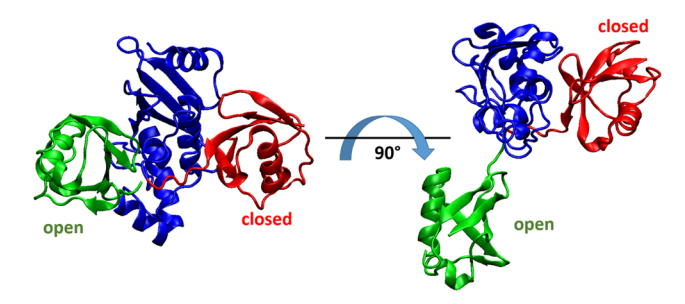


Figure 2. Superimposed Ubc13~Ub complexes in the open and closed positions. The blue structure represents Ubc13, red represents Ub in the closed position, and green represents Ub in the open position. The right structure is rotated 90° with respect to the left. The open structure came from pdb file 2GMI, and the closed structure came from 5AIT. The pbds were superimposed, and the Ubc13 in each pdb was aligned. To improve clarity, the RING E3 and UEV were removed from the figure, and only one Ubc13 is shown.

the effect of the E3 by comparing the thioester strain in the closed complex when the E3 is present to the strain when the E3 is absent. Finally, we measure the how the hydrogen-bonding environment in the active site differs between the closed and open positions. In particular, we focus on the behavior of a highly conserved asparagine in the E2 that may stabilize a reaction intermediate $^{3,20,26-29}$ or may help preorganize the substrates. $^{30-32}$

2. METHODOLOGY

2.1. Structural Preparation. The initial geometries of the Ubc13-Ub complexes were generated from two crystal structures deposited in the RCSB data bank: pdb codes 2GMI and 5AIT. There are two major differences between 2GMI and 5AIT: The Ubc13-Ub complex in 2GMI is in the open position and lacks a RING E3 ligase, whereas the Ubc13-Ub complex in 5AIT is in the closed position and has a RING E3 ligase, specifically the RNF4 RING domain. Figure 2 illustrates the difference between the open and closed conformations. Three initial systems were prepared: 2GMI, 5AIT-noE3, and 5AIT. Only one monomer (chains A–D) was retained in 5AIT, and the E3 (chain A) was also removed in 5AIT-noE3. The noncatalytic, UEV (MMS2 in 2GMI and Ube2 V2 in 5AIT) remained in all three structures. Substituted residue names were changed, and their side-chain atoms were deleted. Specifically, in both crystal structures, C87 in Ubc13 was mutated (lysine in 5AIT and serine in 2GMI). Our simulations used the wild-type cysteine. The LEaP program³³ was used to generate missing atoms. The final structures are shown in Figures S1-S3 in the Supporting Information.

2.2. Thioester Force Field Parametrization. In each structure, the Ub is covalently linked to Ubc13 via a thioester bond, which needs a parameter set. We developed the

parameters using the protocol outlined in refs 31 and 32. Briefly, we generated partial atomic charges by removing the residues that form the thioester linkage between the Ubc13 and Ub from pdb 2GMI (C87 on Ubc13 and G76 on Ub) and capped them with acetyl (ACE) and *N*-methylamide (NME) groups. The charges were then calculated using the RESP protocol.³⁴ The cysteine residue within the thioester was labeled as the AMBER residue CYX, the thioester glycine was labeled as CGLY, and the thioester bond between them was described using parameters from the General AMBER Force Field (GAFF).³⁵

To ensure that our analysis correctly captured the behavior of the thioester strain, we improved upon our previous protocol by parametrizing an explicit out-of-plane bend (improper torsion) for the thioester bond. We added and fit this term against density functional theory (DFT). We used the M06-2X/def2TZVP level of theory. For an initial geometry, we randomly selected a snapshot from one of our simulations and excised the thioester formed between the C-terminal glycine and the cysteine side chain. We capped the dangling peptide bonds using ACE and NME residues (see Figure 3A). Next, we fully optimized the

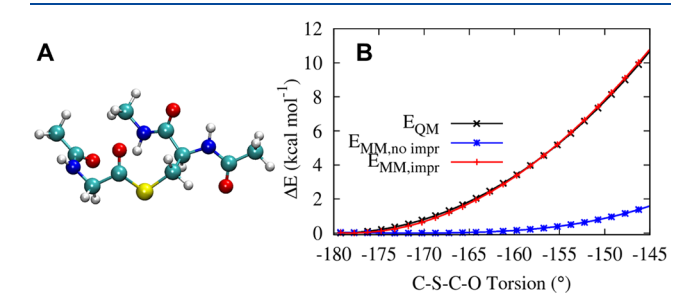


Figure 3. Model used to calculate the stiffness of the out-of-plane-bend in the thioester (A) and comparison of M06-2X/def2TZVP (QM), uncorrected ff12SB (MM), and corrected MM energies (B). In (A), carbon atoms are cyan, nitrogen atoms are blue, oxygen atoms are red, the sulfur atom is yellow, and hydrogen atoms are white. In (B), the black curve shows the QM energies ($E_{\rm QM}$), the blue curve shows the MM energies without an explicit improper term ($E_{\rm MM,no~impr}$), and the red curve shows the MM energies with the added improper torsion ($E_{\rm MM,impr}$).

structures using DFT and Gaussian $09.^{36}$ Finally, we held the heavy atoms fixed and ran a relaxed scan of the thioester bend defined between the C-S-C-O atoms, where S-C-O are all bonded together as required by the AMBER format. Keeping the heavy atoms fixed eliminated changes in energy due to bond stretch, bond angle, torsion, and nonbonded terms. We scanned from -178.7° (fully relaxed) to -146.3° using an increment of 0.5° . We recalculated the energies of the final geometries along the scan using the ff12SB force field, including our custom thioester parameters. We developed the improper torsion term

by fitting the difference between the M06-2X/def2TZVP and ff12SB energy curves to eq 1, where ϕ is the torsion angle and K is the fit parameter:

$$V(\phi) = K[1 + \cos(2\phi - \pi)] \tag{1}$$

The fit was performed using the nonlinear least-squares fit utility in gnuplot4.6.³⁷ The rms of the residuals of the fit was 0.129 kcal mol⁻¹. The results are shown in Figure 3B.The full parameter set for the thioester bond can be found in the SI.

2.3. Molecular Dynamics. All MD was performed using the Amberff12SB force field 38 and the GPU-accelerated PMEMD module in the Amber14 33 and Amber20 39 packages. The structures for 2GMI and 5AIT were solvated in a rectilinear box (r = 12.0 Å) of TIP3P water molecules 40,41 and neutralized with K⁺ and Cl⁻ ions (13 K⁺ and 10 Cl⁻ ions for 2GMI and 10 K⁺, 10 Cl⁻ for 5AIT without the E3, and 12 K⁺ and 20 Cl⁻ for 5AIT with the E3). The systems were stabilized by an optimization, heated to 200 K, and subjected to density equilibration (100 ps, with a time step of 0.5 fs). The systems were then simulated at 300 K for 100 ns using a Langevin thermostat with a collision frequency of 2 ps⁻¹ and a time step of 2 fs. The cutoff for nonbonded interactions structure was 8 Å, and all covalent bonds to hydrogen atoms were held fixed using the SHAKE algorithm. A full microsecond of simulation data was collected for each of the 2GMI, 5AIT-noE3, and 5AIT-E3 structures. Each microsecond simulation was constructed from 10, independent, 100 ns NVT simulations, which can improve sampling.⁴² Snapshots were saved every 2 ps. Trajectory analyses were conducted using CPPTRAJ⁴³ included in AmberTools14³³ and AmberTools21.39 All Amber input files and backbone RMSD plots are included in the SI.

2.4. Density Functional Theory. DFT was used to calculate the stiffness of the thioester when it is bent out-of-plane. Our model thioester was prepared as described in the Thioester Force Field Parametrization subsection and is shown in Figure 3A. Also as previously described, we performed a relaxed scan with heavy atoms fixed. Here, though, we scanned the out-of-plane bend described in Figure 4A from -0.815° (fully relaxed and planar) to 34.18° using an increment of 0.5°. These calculations were performed at the M06-2X/def2TZVP level of theory using the Gaussian 09 suite of programs. ³⁶ All Gaussian input files are included in the SI.

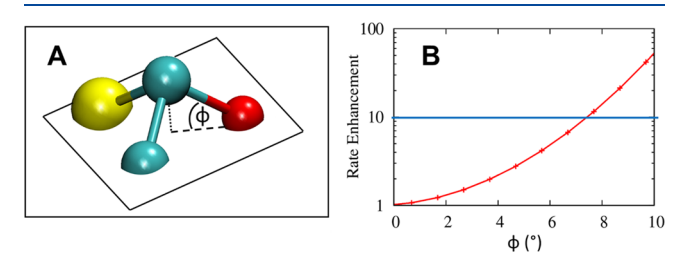


Figure 4. Definition of the C–S–O–C out-of-plane bend ϕ (A), and plot of the rate increase (k_2/k_1) as a function of out-of-plane bend (B). In (A), carbon atoms are cyan, nitrogen atoms are blue, oxygen atoms are red, the sulfur atom is yellow, and hydrogen atoms are white. As shown in (A), the out-of-plane bend is defined so that the last two atoms (O–C) are bonded. The intersection of the blue line and red curve in (B) shows that bending the thioester between 7° and 8° out of plane will increase the rate by a factor of 10. This corresponds to lowering the reaction barrier by 1.0–1.5 kcal mol⁻¹ (see eq 2).

3. RESULTS AND DISCUSSION

3.1. DFT Calculations Show That the Strain Hypothesis Is Reasonable. Kinetics studies show that the presence of a RING E3 enhances the rate of ubiquitination by an E2 by about a factor of 10. 11,30 One hypothesis for the enhancement is that the RING E3 bends the thioester out of plane. Because the carbonyl carbon on the thioester changes from planar to tetrahedral during the first step of the ubiquitination reaction, bending the thioester out of plane will increase the energy of the reactants relative to the transition state, thereby decreasing the activation energy. We tested the feasibility of this hypothesis using a combination of transition-state theory (TST) and DFT calculations.

First, we used eq 2, which is derived from the TST rate expression, to estimate that at room temperature, the reaction barrier should decrease by 1-1.5 kcal mol⁻¹ to increase the rate 10-fold:

$$\Delta \Delta G^{\ddagger} = -RT \ln \left(\frac{k_2}{k_1} \right) \tag{2}$$

where $\Delta\Delta G^{\ddagger} = \Delta G_2^{\ddagger} - \Delta G_1^{\ddagger}$ and is the change in energy barrier, ΔG_2^{\ddagger} is the energy barrier in the presence of the RING E3, ΔG_1^{\ddagger} is the energy barrier in the absence of the RING E3, k_2/k_1 is the ratio of reaction rates for the catalyzed to uncatalyzed reaction, R is the universal gas constant, and T is temperature. In this case, the change in the energy barrier does not originate in lowering the transition-state energy. Instead, the barrier decreases because the strain on the thioester increases the reactant energy.

Next, we used DFT (M06-2X/def2TZVP) to estimate how far out of plane the thioester needs to bend to increase its energy by $1-1.5~{\rm kcal~mol^{-1}}$. To simplify the calculation, we used a model thioester and assumed the change in electronic energy would dominate the change in free energy ($\Delta\Delta G^{\pm}$), that is, we ignored vibrational and rotational enthalpy and entropy contributions. We scanned the C–S–O–C out-of-plane bend for the model thioester (see Methodology), and our calculations show that bending the thioester $7-8^{\circ}$ out-of-plane increases the reactant energy by $1.0-1.5~{\rm kcal~mol^{-1}}$ (see Figure 4B). This is a modest amount of bend, which suggests that the strain hypothesis is reasonable.

3.2. MD Simulations Show That the Closed Ubc13~Ub Is Strained. We analyzed our MD simulations of Ubc13~Ub/E3 complexes to determine if the presence of the E3 strained the thioester linkage in a way that is consistent with experimental observations and our DFT calculations. We examined three models: an open structure (2GMI), a closed structure without the E3 (5AIT-noE3), and a closed structure with the E3 (5AIT). We monitored the out-of-plane bend of the carbonyl carbon in the thioester during our simulations. Each structure was simulated with 10 independent, 100 ns trajectories. Our results are shown in Figure 5.

On average, there is little difference between 2GMI, 5AIT-noE3, and 5AIT. This result is displayed in Table 1 and in Figure 5A. Although the mean angle is slightly elevated in the closed systems (1.2°/1.3° in 5AIT-noE3/5AIT) versus the open system (0.044° in 2GMI), there is significant overlap in the distributions as is clear from Figure 5A. Examined from a different perspective, Table 1 also shows that the average out-of-plane energies ($\langle E_{\rm OPB} \rangle$) for each system are identical. However, since catalysis is a rare event, it is important to examine the extreme ends (the tails) of the distribution. Therefore, we calculated the percent of the trajectory when $E_{\rm OPB}$ was >1.0 and

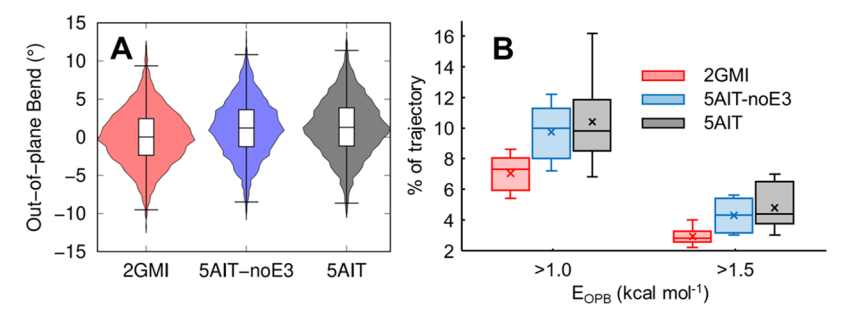


Figure 5. Violin plot (A) of out-of-plane bend and box plot (B) of percent of the trajectory with an out-of-plane bend energy (E_{OPB}) >1.0 and 1.5 kcal mol⁻¹. In both figures, 2GMI (open) is in red, SAIT-noE3 (closed) is in blue, and 5AIT (closed) is in gray. The violin plot indicates that the distribution of out-of-plane bend angles is roughly normal and that the mean and deviations of all three simulations are similar. However, (B) clearly shows that when the Ubc13~Ub conjugate is in the closed position, the thioester experiences a higher out-of-plane bend energy for a greater percentage of the trajectory. In both plots, the boxes indicate the first quartile, the median, and the third quartile. The whiskers indicate 1.5 times the interquartile range.

Table 1. Average out-of-Plane Bend Angle (\langle angle \rangle) and Energy ($\langle E_{OPB} \rangle$) of 2GMI, 5AIT-noE3, and 5AIT^a

	$\langle angle \rangle^b$	$\langle E_{\mathrm{OPB}} \rangle^{b}$	$E_{\rm OPB} > 1.0^{\circ}$ (%)	$E_{\text{OPB}} > 1.5^{c}$ (%)
2GMI	0.044 ± 3.6	0.31 ± 0.45	7.0 ± 1.1	2.9 ± 0.51
5AIT-noe3	1.2 ± 3.7	0.36 ± 0.49	9.7 ± 1.7	4.3 ± 0.96
5AIT	1.3 ± 3.7	0.38 ± 0.52	10.4 ± 2.5	4.8 ± 1.4

^aThe last columns show the percentage of the simulations where the strain energy is >1.0 kcal mol⁻¹ and 1.5 kcal mol⁻¹. All energies are in kcal mol⁻¹, and all angles are in degrees. ^bThe error is calculated as the standard error over the entire 1 μ s data set. ^cThe error is calculated as the standard error over 10 simulations.

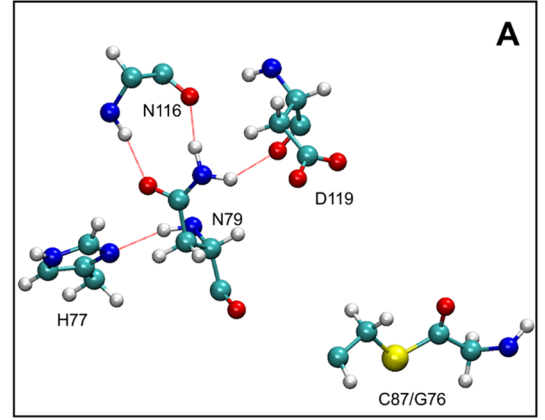
 $1.5 \text{ kcal mol}^{-1}$ —the amount of strain energy required to account for the RING E3-induced rate increase. The results are displayed in Table 1 and Figure 5B.

The final columns in Table 1 show that there is more out-of-plane bend energy in the closed systems (5AIT-noE3/5AIT) than the open system (2GMI). In fact, $E_{\rm OPB}$ is >1.0 kcal mol⁻¹ for 9.7%/10.4% of the trajectory and >1.5 kcal mol⁻¹ for 4.3%/4.8% of the trajectory in the closed systems. For 2GMI, these numbers are significantly smaller, 7.0% and 2.9%. The box plots in Figure 5B also indicate that there is very little overlap between

the open and closed systems and the overall distribution for the closed systems skews much higher than the open system. Interestingly, the presence of the E3 seems to not make much of a difference; there is a similar amount of $E_{\rm OPB}$ in SAIT-noE3 and SAIT.

3.3. MD Simulations Show That the Closed Ubc13~Ub Has a More Rigid Binding Pocket. We also examined the hydrogen-bonding properties of the binding pocket and the flexibility of the thioester. Specifically, we observed the hydrogen-bonding partners of the asparagine (N79 in Ubc13) that is located within the highly conserved HPN motif found in E2 enzymes.²⁸ N79 has been hypothesized to stabilize the zwitterionic, tetrahedral intermediate of the ubiquitination reaction.^{3,20,26} Alternately, our group, along with some others, have hypothesized that this asparagine stabilizes an active site loop to preorganize the thioester.^{30–32} This preorganization keeps the thioester rigid, allowing it to more easily achieve a reactive configuration. Therefore, we examined how the open/closed Ubc13~Ub state affects the hydrogen bonding in the active site, and we examined if the presence of the E3 had an effect. Our results are shown in Figures 6 and 7.

Figure 6A,B shows the typical hydrogen-bonding environment in the active site for both open and closed systems,



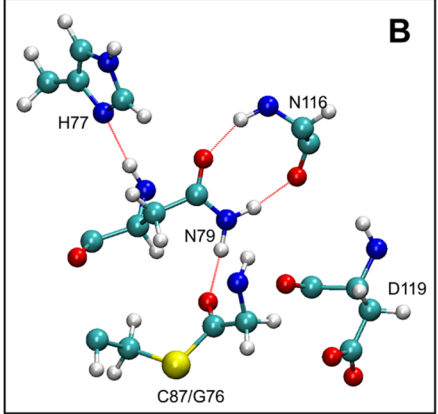


Figure 6. Typical hydrogen-bonding environments of 2GMI (A) and 5AIT-noE3/5AIT (B). All residues are from Ubc13, except G76, which is in Ub. In (A) and (B), carbon atoms are cyan, nitrogen atoms are blue, oxygen atoms are red, the sulfur atom is yellow, hydrogen atoms are white, and hydrogen bonds are red, dotted lines. Both Ubc13~Ub configurations show persistent hydrogen bonding between the side chain of N79 and the backbone of N116 and persistent hydrogen bonding between the side chain of H77 and the backbone of N79. In the open configuration (2GMI, A), there is no significant hydrogen bonding between N79 and the thioester, C87/G76. The hydrogen bonding increases dramatically when Ubc13~Ub is in the closed position (5AIT-noE3/5AIT, B).

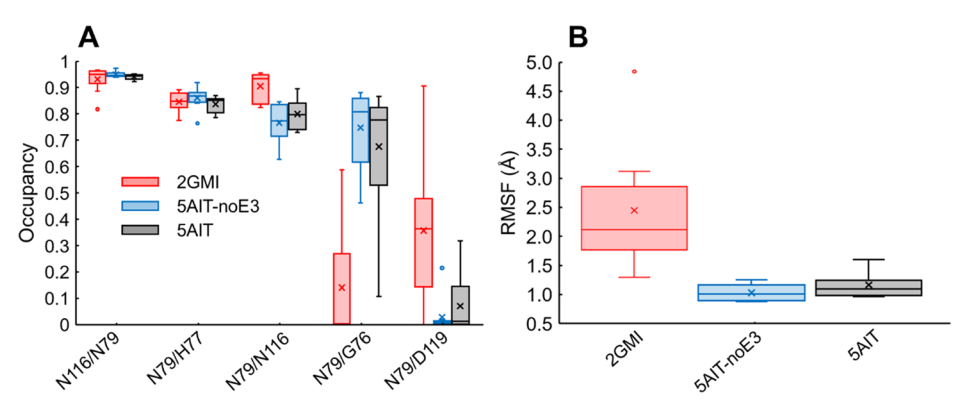


Figure 7. These box plots describes the hydrogen-bonding environment of the active site pocket in Ubc13 (A) and the fluctuations of the thioester bond (B). In each figure, 2GMI data is red, 5AIT-noE3 is blue, and 5AIT is gray. When the Ubc13~Ub conjugate is in the closed position (5AIT-noE3/5AIT), the N79/G76 hydrogen bond is populated and the thioester fluctuates less. In both plots, the boxes indicate the first quartile, the median, and the third quartile. The whiskers indicate 1.5 times the interquartile range, and the points represent outliers.

respectively. Both positions show significant hydrogen bonding between the side chain of N79 and the backbone of N116 and significant hydrogen bonding between the side chain of H77 and the backbone of N79. We note that this last hydrogen bond is not seen in the crystal structure, ²⁰ since the delta nitrogen on the imidazole ring in H77 is rotated away from the backbone of N79. The orientation shown in Figure 6 is confirmed by NMR^{28,44} studies and electronic structure calculations.³¹ However, when Ubc13~Ub is open, there is negligible hydrogen bonding between N79 and the thioester (the carbonyl oxygen on G76). In the closed state, this hydrogen bond is populated. These observations are quantified in Figure 7A.

The boxplot in Figure 7A shows that there is consistent hydrogen bonding between N79, N116, and H77, but the N79/G76 hydrogen bond population depends on the state of the system (open versus closed). The average occupancy for the N79/G76 hydrogen bond is 0.14 ± 0.07 in 2GMI (open), 0.75 ± 0.05 in 5AIT-noE3 (closed), and 0.68 ± 0.08 in 5AIT (closed). (The error is the calculated standard error over the ten simulations.) The box plots, which show the variance in more detail, show that although 2GMI clearly has a lower N79/G76 population, the variance in all three systems is high, a further indication that this hydrogen bond is weak. We have noted previously that if this hydrogen bond is too strong, it can overstabilize the transition intermediate, which may negatively impact catalysis.

Finally, we calculated the fluctuations of the thioester in all three systems (see Figure 7B). First, we aligned the backbone of the entire protein for the trajectory, then measured the RMSF of the thioester using CPPTRAJ. 43 The thioester is clearly more rigid when Ubc13~Ub is in the closed state. In 5AIT-noE3 and 5AIT, the RMSFs of the thioester are 1.03 \pm 0.05 Å and 1.16 \pm 0.08 Å. In the open, 2GMI simulation, the RMSF is 2.45 ± 0.33 Å. This pattern makes sense, since the hydrogen bond that holds the thioester in place (N79/G76) is weak in 5AIT/5AIT-noE3 and even weaker in 2GMI. The observation that the more rigid binding pocket corresponds to the more reactive enzyme structure supports the hypothesis that the N79 hydrogen bond preorganizes the thioester, allowing it to more easily form a reactive interaction with the substrate lysine. Interestingly, there is little difference between 5AIT-noE3 and 5AIT, which further indicates that the E3 is a passive actor in the ubiquitination reaction and activates Ub transfer by promoting the Ubc13~Ub closed state.

4. DATA AND SOFTWARE AVAILABILITY

The software used for MD simulations is AMBER14 and AMBER20 available at http://ambermd.org/. The DFT calculations were performed using Gaussian09, revD01 available at https://gaussian.com/. Least squares fitting for the thioester improper torsion was performed using gnuplot4.6 available at http://www.gnuplot.info/. Trajectory analyses were performed using the CPPTRAJ modules in the AmberTools14 and AmberTools21 available at https://ambermd.org/. AmberTools.php. The AMBER input and parameter files for the MD simulations and Gaussian 09 input files for the thioester improper torsion parametrization are freely accessible as part of the SI. Due to their large size, full MD trajectories are available upon request.

5. CONCLUSION

It is known that the presences of a RING E3 ligase increases the efficiency of E2-catalyzed ubiquitination. However, the source of this effect is unknown. Our MD simulations support the hypothesis that when the E3 puts the E2~Ub complex into the closed position, it puts tension on the thioester bond, making it easier to break.⁶

We examined three model E2~Ub complexes: an open confirmation without the E3 (2GMI), a closed conformation without the E3 (5AIT-noE3), and a closed confirmation with the E3 (5AIT). We monitored the out-of-plane bend of the thioester linking the E2, Ubc13, and Ub and found that this bend is greater in the closed position than in the open. We note that although the average bend is similar across all models, the tail ends of the distribution differ. The closed systems are more likely to experience a high out-of-plane bend than the open system. Interestingly, the presence of the E3 had no effect. This implies that the E3 functions in part by promoting the closed position, but does not play an active catalytic role.

Next, we measured the flexibility and hydrogen-bonding environment of the active site. We saw that the thioester fluctuates less and there is more hydrogen bonding when Ubc13~Ub is closed. When the thioester is held fixed, it can help preorganize the active site, improving catalytic efficiency. Once again, the presence of the E3 had no effect on the hydrogen-bond population, which provides more evidence for a passive role for the E3.

Finally, we note that this study only measures the effect of the RING E3 indirectly. In other words, we did not calculate

reaction rates of ubiquitination in the presence and absence of the RING E3. Because we used nonreactive force-fields, we could not simulate chemical reactions, that is, bond breaking and forming nor did we examine the free energy difference between the open and closed configurations. Understanding how this free energy change may shift in the presence of a RING E3 and how it is coupled to the thioester activation will lead to a more thorough understanding of how the RING E3 aids in ubiquitination. We also note that reaction enhancement of the RING E3 $(\sim 10 \times)^{11,30}$ is much smaller compared to the enhancement of the E2 $(\sim 10^8 \times)$, 45,46 meaning the RING E3 mechanism is more subtle than the electrostatic stabilization of transition states mechanism typically used by enzymes. 47,48 Placing a bond under slight strain is an example of a subtle enzymatic strategy and may explain why the Ub transfer exclusively from the closed position and why that configuration is promoted by the RING E3 for Ub and other Ubl conjugating enzymes.

ASSOCIATED CONTENT

Solution Supporting Information

The Supporting Information is available free of charge at https://pubs.acs.org/doi/10.1021/acs.jcim.2c00423.

Figures depicting the model systems (2GMI, 5AIT-noE3, and 5AIT); custom force field parameters for the thioester bond, including partial charges and the improper torsion; backbone RMSDs; and the SI cites refs 13, 35, and 38 (PDF)

AMBER input and parameter files for the MD simulations and Gaussian 09 input files for the thioester improper torsion parametrization (ZIP)

AUTHOR INFORMATION

Corresponding Author

Isaiah Sumner – Department of Chemistry and Biochemistry, James Madison University, Harrisonburg, Virginia 22807, United States; orcid.org/0000-0002-1422-5476; Email: sumneric@jmu.edu

Author

Jay-Anne K. Johnson – Department of Chemistry and Biochemistry, James Madison University, Harrisonburg, Virginia 22807, United States

Complete contact information is available at: https://pubs.acs.org/10.1021/acs.jcim.2c00423

Author Contributions

I.S. conceived and supervised the study and designed the experiments. J.K.J. and I.S. conducted the experiments and wrote the manuscript.

Notes

The authors declare no competing financial interest.

ACKNOWLEDGMENTS

The authors of this manuscript are committed to supporting and advancing women in chemistry. This material is based upon work supported by the National Science Foundation under grant no. CHE-1757874. Computational resources were provided in part by the MERCURY consortium (http://mercuryconsortium.org/) under NSF grants CHE-1229354, CHE-1662030, and CHE-2018427.

REFERENCES

- (1) Pickart, C. M.; Eddins, M. J. Ubiquitin: Structures, Functions, Mechanisms. *Biochim. Biophys. Acta Mol. Cell Res.* **2004**, *1695* (1–3), 55–72.
- (2) Kerscher, O.; Felberbaum, R.; Hochstrasser, M. Modification of Proteins by Ubiquitin and Ubiquitin-Like Proteins. *Annu. Rev. Cell Dev. Biol.* **2006**, 22 (1), 159–180.
- (3) Wenzel, D. M.; Stoll, K. E.; Klevit, R. E. E2s: Structurally Economical and Functionally Replete. *Biochem. J.* **2011**, 433, 31–42.
- (4) Richard, T. J. C.; Herzog, L. K.; Vornberger, J.; Rahmanto, A. S.; Sangfelt, O.; Salomons, F. A.; Dantuma, N. P. K63-Linked Ubiquitylation Induces Global Sequestration of Mitochondria. *Sci. Rep* **2020**, *10* (1), 22334.
- (5) Berndsen, C. E.; Wolberger, C. New Insights into Ubiquitin E3 Ligase Mechanism. *Nat. Struct Mol. Biol.* **2014**, 21 (4), 301–307.
- (6) Plechanovová, A.; Jaffray, E. G.; Tatham, M. H.; Naismith, J. H.; Hay, R. T. Structure of a RING E3 Ligase and Ubiquitin-Loaded E2 Primed for Catalysis. *Nature* **2012**, 489 (7414), 115–120.
- (7) Li, W.; Bengtson, M. H.; Ulbrich, A.; Matsuda, A.; Reddy, V. A.; Orth, A.; Chanda, S. K.; Batalov, S.; Joazeiro, C. A. P. Genome-Wide and Functional Annotation of Human E3 Ubiquitin Ligases Identifies MULAN, a Mitochondrial E3 That Regulates the Organelle's Dynamics and Signaling. *PLoS One* **2008**, *3* (1), No. e1487.
- (8) Metzger, M. B.; Pruneda, J. N.; Klevit, R. E.; Weissman, A. M. RING-Type E3 Ligases: Master Manipulators of E2 Ubiquitin-Conjugating Enzymes and Ubiquitination. *Biochim. Biophys. Acta-Mol. Cell Res.* **2014**, *1843* (1), 47–60.
- (9) Saha, A.; Lewis, S.; Kleiger, G.; Kuhlman, B.; Deshaies, R. J. Essential Role for Ubiquitin-Ubiquitin-Conjugating Enzyme Interaction in Ubiquitin Discharge from Cdc34 to Substrate. *Mol. Cell* **2011**, 42 (1), 75–83.
- (10) Pruneda, J. N.; Stoll, K. E.; Bolton, L. J.; Brzovic, P. S.; Klevit, R. E. Ubiquitin in Motion: Structural Studies of the Ubiquitin-Conjugating Enzyme-Ubiquitin Conjugate. *Biochemistry* **2011**, *50* (10), 1624–1633.
- (11) Pruneda, J. N.; Littlefield, P. J.; Soss, S. E.; Nordquist, K. A.; Chazin, W. J.; Brzovic, P. S.; Klevit, R. E. Structure of an E3:E2~Ub Complex Reveals an Allosteric Mechanism Shared among RING/U-Box Ligases. *Mol. Cell* **2012**, *47* (6), 933–942.
- (12) Dou, H.; Buetow, L.; Sibbet, G. J.; Cameron, K.; Huang, D. T. Structure of BIRC7–E2 Ubiquitin Conjugate Reveals the Mechanism of Ubiquitin Transfer by a RING Dimer. *Nat. Struct. Mol. Biol.* **2012**, *19* (9), 876.
- (13) Page, R. C.; Pruneda, J. N.; Amick, J.; Klevit, R. E.; Misra, S. Structural Insights into the Conformation and Oligomerization of E2~Ubiquitin Conjugates. *Biochemistry* **2012**, *51* (20), 4175–4187.
- (14) Soss, S. E.; Klevit, R. E.; Chazin, W. J. Activation of UbcH5c—Ub Is the Result of a Shift in Interdomain Motions of the Conjugate Bound to U-Box E3 Ligase E4B. *Biochemistry* **2013**, *52* (17), 2991–2999.
- (15) Branigan, E.; Plechanovová, A.; Jaffray, E. G.; Naismith, J. H.; Hay, R. T. Structural Basis for the RING-Catalyzed Synthesis of K63-Linked Ubiquitin Chains. *Nat. Struct. Mol. Biol.* **2015**, 22, 597.
- (16) Branigan, E.; Carlos Penedo, J.; Hay, R. T. Ubiquitin Transfer by a RING E3 Ligase Occurs from a Closed E2~Ubiquitin Conformation. *Nat. Commun.* **2020**, *11* (1), 2846.
- (17) Nakasone, M. A.; Majorek, K. A.; Gabrielsen, M.; Sibbet, G. J.; Smith, B. O.; Huang, D. T. Structure of UBE2K—Ub/E3/PolyUb Reveals Mechanisms of K48-Linked Ub Chain Extension. *Nat. Chem. Biol.* **2022**, *18*, 422.
- (18) Scott, D. C.; Sviderskiy, V. O.; Monda, J. K.; Lydeard, J. R.; Cho, S. E.; Harper, J. W.; Schulman, B. A. Structure of a RING E3 Trapped in Action Reveals Ligation Mechanism for the Ubiquitin-like Protein NEDD8. *Cell* **2014**, *157* (7), 1671–1684.
- (19) Streich, F. C., Jr; Lima, C. D. Capturing a Substrate in an Activated RING E3/E2-SUMO Complex. *Nature* **2016**, *536* (7616), 304–308.
- (20) Eddins, M. J.; Carlile, C. M.; Gomez, K. M.; Pickart, C. M.; Wolberger, C. Mms2-Ubc13 Covalently Bound to Ubiquitin Reveals

- the Structural Basis of Linkage-Specific Polyubiquitin Chain Formation. *Nat. Struct. Mol. Biol.* **2006**, *13* (10), 915–920.
- (21) Zhao, S.; Ulrich, H. D. Distinct Consequences of Posttranslational Modification by Linear versus K63-Linked Polyubiquitin Chains. *Proc. Natl. Acad. Sci.* **2010**, *107* (17), 7704–7709.
- (22) Nathan, J. A.; Tae Kim, H.; Ting, L.; Gygi, S. P.; Goldberg, A. L. Why Do Cellular Proteins Linked to K63-Polyubiquitin Chains Not Associate with Proteasomes? *EMBO J.* **2013**, 32 (4), 552–565.
- (23) Deng, L.; Wang, C.; Spencer, E.; Yang, L.; Braun, A.; You, J.; Slaughter, C.; Pickart, C.; Chen, Z. J. Activation of the IkB Kinase Complex by TRAF6 Requires a Dimeric Ubiquitin-Conjugating Enzyme Complex and a Unique Polyubiquitin Chain. *Cell* **2000**, *103* (2), 351–361.
- (24) Ulrich, H. D. Regulating Post-Translational Modifications of the Eukaryotic Replication Clamp PCNA. *DNA Repair* (*Amst*) **2009**, 8 (4), 461–469.
- (25) Wang, G.; Gao, Y.; Li, L.; Jin, G.; Cai, Z.; Chao, J.-I; Lin, H.-K. K63-Linked Ubiquitination in Kinase Activation and Cancer. *Frontiers in Oncology* **2012**, *2*, 00005.
- (26) Wu, P. Y.; Hanlon, M.; Eddins, M.; Tsui, C.; Rogers, R. S.; Jensen, J. P.; Matunis, M. J.; Weissman, A. M.; Wolberger, C. P.; Pickart, C. M. A Conserved Catalytic Residue in the Ubiquitin-Conjugating Enzyme Family. *EMBO J.* **2003**, 22 (19), 5241–5250.
- (27) Markin, C. J.; Saltibus, L. F.; Kean, M. J.; McKay, R. T.; Xiao, W.; Spyracopoulos, L. Catalytic Proficiency of Ubiquitin Conjugation Enzymes: Balancing p k a Suppression, Entropy, and Electrostatics. *J. Am. Chem. Soc.* **2010**, 132 (50), 17775–17786.
- (28) Cook, B. W.; Shaw, G. S. Architecture of the Catalytic HPN Motif Is Conserved in All E2 Conjugating Enzymes. *Biochem. J.* **2012**, 445 (2), 167–174.
- (29) Zhen, Y.; Qin, G.; Luo, C.; Jiang, H.; Yu, K.; Chen, G. Exploring the RING-Catalyzed Ubiquitin Transfer Mechanism by MD and QM/MM Calculations. *PLoS One* **2014**, *9* (7), e101663.
- (30) Berndsen, C. E.; Wiener, R.; Yu, I. W.; Ringel, A. E.; Wolberger, C. A Conserved Asparagine Has a Structural Role in Ubiquitin-Conjugating Enzymes. *Nat. Chem. Biol.* **2013**, 9 (3), 154–156.
- (31) Wilson, R. H.; Zamfir, S.; Sumner, I. Molecular Dynamics Simulations Reveal a New Role for a Conserved Active Site Asparagine in a Ubiquitin-Conjugating Enzyme. *J. Mol. Graph. Model* **2017**, *76*, 403.
- (32) Jones, W. M.; Davis, A. G.; Wilson, R. H.; Elliott, K. L.; Sumner, I. A Conserved Asparagine in a Ubiquitin-Conjugating Enzyme Positions the Substrate for Nucleophilic Attack. *J. Comput. Chem.* **2019**, 40 (22), 1969.
- (33) Case, D. A.; Babin, V.; Berryman, J. T.; Betz, R. M.; Cai, Q.; Cerutti, D. S.; Cheatham, T. I.; Darden, T. A.; Duke, R. E.; Gohlke, H.; Goetz, A. W.; Gusarov, S.; Homeyer, N.; Janowski, P.; Kaus, J.; Kolossváry, I.; Kovalenko, A.; Lee, T. S.; LeGrand, S.; Luchko, T.; Luo, R.; Madej, B.; Merz, K. M.; Paesani, F.; Roe, D. R.; Roitberg, A.; Sagui, C.; Salomon-Ferrer, R.; Seabra, G.; Simmerling, C. L.; Smith, W.; Swails, J.; Walker, R. C.; Wang, J.; Wolf, R. M.; Wu, X.; Kollman, P. A. AMBER 14; University of California: San Francisco, CA, 2014.
- (34) Bayly, C. I.; Cieplak, P.; Cornell, W.; Kollman, P. A. A Well-Behaved Electrostatic Potential Based Method Using Charge Restraints for Deriving Atomic Charges: The RESP Model. *J. Phys. Chem.* **1993**, *97* (40), 10269–10280.
- (35) Wang, J.; Wolf, R. M.; Caldwell, J. W.; Kollman, P. A.; Case, D. A. Development and Testing of a General Amber Force Field. *J. Comput. Chem.* **2004**, 25 (9), 1157–1174.
- (36) Frisch, M. J.; Trucks, G. W.; Schlegel, H. B.; Scuseria, G. E.; Robb, M. A.; Cheeseman, J. R.; Scalmani, G.; Barone, V.; Mennucci, B.; Petersson, G. A.; Nakatsuji, H.; Caricato, M.; Li, X.; Hratchian, H. P.; Izmaylov, A. F.; Bloino, J.; Zheng, G.; Sonnenberg, J. L.; Hada, M.; Ehara, M.; Toyota, K.; Fukuda, R.; Hasegawa, J.; Ishida, M.; Nakajima, T.; Honda, Y.; Kitao, O.; Nakai, H.; Vreven, T.; Montgomery, J. A., Jr.; Peralta, J. E.; Ogliaro, F.; Bearpark, M.; Heyd, J. J.; Brothers, E.; Kudin, K. N.; Staroverov, V. N.; Kobayashi, R.; Normand, J.; Raghavachari, K.; Rendell, A.; Burant, J. C.; Iyengar, S. S.; Tomasi, J.; Cossi, M.; Rega, N.; Millam, J. M.; Klene, M.; Knox, J. E.; Cross, J. B.; Bakken, V.; Adamo,

- C.; Jaramillo, J.; Gomperts, R.; Stratmann, R. E.; Yazyev, O.; Austin, A. J.; Cammi, R.; Pomelli, C.; Ochterski, J. W.; Martin, R. L.; Morokuma, K.; Zakrzewski, V. G.; Voth, G. A.; Salvador, P.; Dannenberg, J. J.; Dapprich, S.; Daniels, A. D.; Farkas, O.; Foresman, J. B.; Ortiz, J. V.; Cioslowski, J.; Fox, D. J. *Gaussian 09*, revisions E.01 and B.01; Gaussian, Inc.: Wallingford, CT, 2009.
- (37) Williams, T.; Kelley, C.et al. Gnuplot 4.6: An Interactive Plotting Program, 2013.
- (38) Case, D. A.; Darden, T. A.; Cheatham, T. I.; Simmerling, C. L.; Wang, J.; Duke, R. E.; Luo, R.; Walker, R. C.; Zhang, W.; Merz, K. M.; Roberts, B.; Hayik, S.; Roitberg, A.; Seabra, G.; Swails, J.; Goetz, A. W.; Kolossváry, I.; Wong, K. F.; Paesani, F.; Vanicek, J.; Wolf, R. M.; Liu, J.; Wu, X.; Brozell, S. R.; Steinbrecher, T.; Gohlke, H.; Cai, Q.; Ye, X.; Wang, J.; Hsieh, M.-J.; Cui, G.; Roe, D. R.; Mathews, D. H.; Seetin, M. G.; Salomon-Ferrer, R.; Sagui, C.; Babin, V.; Luchko, T.; Gusarov, S.; Kovalenko, A.; Kollman, and P. A. *AMBER 12*; University of California: San Francisco, CA, 2012.
- (39) Case, D. A.; Aktulga, H. M.; Belfon, K.; Ben-Shalom, I. Y.; Brozell, S. R.; Cerutti, D. S.; Cheatham, T. I.; Cisneros, G. A.; Cruzeiro, V. W. D.; Darden, T. A.; Duke, R. E.; Giambasu, G.; Gilson, M. K.; Gohlke, H.; Goetz, A. W.; Harris, R.; Izadi, S.; Izmailov, S. A.; Jin, C.; Kasavajhala, K.; Kaymak, M. C.; King, E.; Kovalenko, A.; T, K.; Lee, T. S.; LeGrand, S.; Li, P.; Lin, C.; Liu, J.; Luchko, T.; Luo, R.; Machado, M.; Man, V.; Madej, B.; Manathunga, M.; Merz, K. M.; Miao, Y.; Mikhailovskii, O.; Monard, G.; Nguyen, H.; O'Hearn, K. A.; Onufriev, A.; Pan, F.; Pantano, S.; Qi, R.; Rahnamoun, A.; Roe, D. R.; Roitberg, A.; Sagui, C.; Schott-Verdugo, S.; Shen, J.; Simmerling, C. L.; Skrynnikov, N. R.; Smith, J.; Swails, J.; Walker, R. C.; Wang, J.; Wei, H.; Wolf, R. M.; Wu, X.; Xue, Y.; York, D. M.; Zhao, S.; Kollman, P. A. Amber; University of California: San Francisco, CA, 2021.
- (40) Jorgensen, W. L.; Chandrasekhar, J.; Madura, J. D.; Impey, R. W.; Klein, M. L. Comparison of Simple Potential Functions for Simulating Liquid Water. *J. Chem. Phys.* **1983**, *79* (2), 926.
- (41) Mark, P.; Nilsson, L. Structure and Dynamics of the TIP3P, SPC, and SPC/E Water Models at 298 K. J. Phys. Chem. A **2001**, 105 (43), 9954–9960.
- (42) Knapp, B.; Ospina, L.; Deane, C. M. Avoiding False Positive Conclusions in Molecular Simulation: The Importance of Replicas. *J. Chem. Theory Comput* **2018**, *14* (12), 6127–6138.
- (43) Roe, D. R.; Cheatham, T. E. PTRAJ and CPPTRAJ: Software for Processing and Analysis of Molecular Dynamics Trajectory Data. *J. Chem. Theory Comput* **2013**, *9* (7), 3084–3095.
- (44) Putney, D. R.; Todd, E. A.; Berndsen, C. E.; Wright, N. T. Chemical Shift Assignments for S. Cerevisiae Ubc13. *Biomol. NMR Assign* **2015**, *9* (2), 407–410.
- (45) Štrajbl, M.; Florián, J.; Warshel, A. Ab Initio Evaluation of the Free Energy Surfaces for the General Base/Acid Catalyzed Thiolysis of Formamide and the Hydrolysis of Methyl Thiolformate: A Reference Solution Reaction for Studies of Cysteine Proteases. *J. Phys. Chem. B* **2001**, *105* (19), 4471–4484.
- (46) Rout, M. K.; Hodge, C. D.; Markin, C. J.; Xu, X.; Glover, J. N. M.; Xiao, W.; Spyracopoulos, L. Stochastic Gate Dynamics Regulate the Catalytic Activity of Ubiquitination Enzymes. *J. Am. Chem. Soc.* **2014**, 136 (50), 17446–17458.
- (47) Warshel, A. Energetics of Enzyme Catalysis. *Proc. Natl. Acad. Sci.* **1978**, 75 (11), 5250–5254.
- (48) Warshel, A.; Sharma, P. K.; Kato, M.; Xiang, Y.; Liu, H.; Olsson, M. H. M. Electrostatic Basis for Enzyme Catalysis. *Chem. Rev.* **2006**, *106* (8), 3210–3235.